AIAA JOURNAL
Vol. 41, No. 5, May 2003

Pressure-Correction Method for Low-Speed Pressure-Sensitive Paint Measurements

Tianshu Liu*
NASA Langley Research Center, Hampton, Virginia 23681

An iterative pressure-correction method is developed that can be used to recover the incompressible pressure-coefficient distribution from pressure-sensitive paint (PSP) results obtained at two suitably higher subsonic Mach numbers. The pressure-correction method provides an alternative approach to overcome the well-known difficulty of using PSP in low-speed flows. For validation, this method is applied to flows over a circular cylinder, sphere, prolate spheroid, transonic body, and delta wing. Limitations and uncertainty of the pressure-correction method are discussed.

Introduction

PRESSURE–SENSITIVE paint (PSP) is an optical sensor for global pressure measurements based on the oxygen-quenching mechanism of luminescence. PSP is particularly effective in high subsonic, transonic, and supersonic flow regimes. However, PSP measurement in low-speed flows where the Mach number is typically less than 0.3 is a challenging problem because a small pressure change is difficult to be sufficiently resolved by PSP. The major error sources, notably the temperature effect, image misalignment, and charge-coupled device (CCD) camera noise, must be minimized to obtain acceptable quantitative pressure results in low-speed flows. The resolution of PSP measurements is eventually limited by the photon-shot-noise of CCD cameras at low limiting Mach number (Ref. 1). Previous work on low-speed PSP measurements focused on pushing the boundary of instrumentation to the limit to resolve a small pressure change. Using a 14-bit CCD camera and carefully controlling the error sources, Brown[2] obtained reasonably good PSP measurements on a NACA 0012 airfoil at speeds as low as 20 m/s. However, because many error sources are strongly dependent on environmental testing factors, the cautious measures used by Brown in a small wind tunnel cannot be generally applied to PSP measurements in large-production wind tunnels. Some low-speed PSP measurements were conducted on the upper surfaces of delta wings where a relatively large pressure change is induced by leading-edge vortices.[3–5] Using a PSP with low temperature sensitivity, Le Sant et al.[5] measured the pressure distributions on car models at speeds as low as 40 m/s. In general, because PSP is an oxygen sensor, the capability of PSP is severely limited in applications of low-speed aerodynamics, and instrumentation issues are increasingly difficult as the flow velocity decreases. In this paper, we propose a pressure-correction method applied to low-speed PSP measurements without directly addressing the intrinsic difficulty of PSP instrumentation in low-speed flows. This method extrapolates the incompressible pressure coefficient from PSP measurements at higher Mach numbers (Mach 0.3–0.6) by removing the compressibility effect. Although this work is motivated by the difficulty in making PSP measurements at low speeds, the developed method can be applied to other relevant measurements and computations.

Sensitivity

Sensitivity analysis indicates that when the freestream Mach number is increased a small amount, the performance of PSP can be considerably enhanced while the change in the nondimensional pressure coefficient remains small for low Mach numbers. There is a significant difference between the responses of pressure p and the pressure coefficient, $C_p = (2/\gamma M_\infty^2)(p/p_\infty - 1)$, to the freestream Mach number M_∞, where $\gamma = 1.4$ is the specific heat ratio for air. According to the Prandtl–Glauert rule, $C_p = C_{p\text{inc}}/\sqrt{(1 - M_\infty^2)}$, we have an estimate for the pressure coefficient $C_p \approx C_{p\text{inc}}(1 + M_\infty^2/2)$ for $M_\infty^2 \ll 1$, where $C_{p\text{inc}}$ is the pressure coefficient in incompressible flow. The relative sensitivity of the pressure coefficient C_p to the Mach number for $M_\infty^2 \ll 1$ is estimated by

$$S_{C_p} = \frac{M_\infty}{C_p}\frac{\mathrm{d}C_p}{\mathrm{d}M_\infty} \approx M_\infty^2 \tag{1}$$

In contrast, the relative sensitivity of pressure to the Mach number is approximately

$$S_{p-p_\infty} = \frac{M_\infty}{(p - p_\infty)}\frac{\mathrm{d}(p - p_\infty)}{\mathrm{d}M_\infty} \approx 2 \tag{2}$$

For $M_\infty^2 \ll 1$, S_{p-p_∞} is much larger than S_{C_p}. For example, for $M_\infty = 0.3$ and $\mathrm{d}M_\infty/M_\infty = 10\%$, the fractional change of pressure difference is $\mathrm{d}(p - p_\infty)/(p - p_\infty) \approx 20\%$, whereas the fractional change of C_p is only $\mathrm{d}C_p/C_p \approx 0.9\%$. This analysis is supported by pressure measurements on a semispan wing and a high-wing transport model.[6,7]

Clearly, PSP can take advantage of the relative insensitivity of the pressure coefficient C_p to the Mach number to achieve the initial approximate incompressible pressure-coefficient distribution from suitably higher-Mach-number data. Furthermore, the compressibility effect for C_p can be corrected by using the classical and proposed pressure-correction methods. The classical pressure-correction formulas are normally applicable to two-dimensional and axisymmetrical flows. In this paper, we develop an iterative pressure-correction method for general three-dimensional flows, allowing recovery of the incompressible pressure coefficient $C_{p\text{inc}}$ from PSP measurements at two different subsonic Mach numbers. For validation, the iterative pressure-correction method is applied to flows over a circular cylinder, sphere, prolate spheroid, transonic body, and delta wing.

Classical Pressure-Correction Formulas

Historically, the pressure-correction formulas were derived to extrapolate the pressure coefficient to subsonic compressible flows from incompressible flow theory and low-speed pressure measurements. In contrast, for PSP application, the pressure-correction formulas are used to transform the compressible pressure coefficient C_p to the corresponding incompressible pressure coefficient $C_{p\text{inc}}$. The theoretical foundation for pressure correction in two-dimensional potential flows is well established. The linearized theory for subsonic compressible flow gives the Prandtl–Glauert rule (see Refs. 8 and 9)

Received 21 May 2002; revision received 22 November 2002; accepted for publication 10 December 2002.

*Research Scientist, Model Systems Branch, Mail Stop 238; t.liu@larc.nasa.gov. Member AIAA.

$$C_p = C_{\text{pinc}} \Big/ \sqrt{1 - M_\infty^2} \tag{3}$$

The Laitone rule with local Mach number correction (see Ref. 8) is

$$C_p = C_{\text{pinc}} \Bigg/ \left\{ \sqrt{1 - M_\infty^2} + \left[\frac{M_\infty^2 \left(1 + [(\gamma - 1)/2] M_\infty^2\right)}{2\sqrt{1 - M_\infty^2}} \right] C_{\text{pinc}} \right\} \tag{4}$$

The use of a hodograph solution of the nonlinear potential equation gives the von Kármán–Tsien rule (see Ref. 8)

$$C_p = C_{\text{pinc}} \Bigg/ \left[\sqrt{1 - M_\infty^2} + \left(\frac{M_\infty^2}{1 + \sqrt{1 - M_\infty^2}} \right) \frac{C_{\text{pinc}}}{2} \right] \tag{5}$$

For $M_\infty^2 \ll 1$, the approximate expressions of the classical pressure-correction formulas are as follows.

Prandtl–Glauert:

$$C_p \approx C_{\text{pinc}} + M_\infty^2 C_{\text{pinc}} \big/ 2 \tag{6a}$$

Laitone:

$$C_p \approx C_{\text{pinc}} + M_\infty^2 C_{\text{pinc}} (1 - C_{\text{pinc}}) \big/ 2 \tag{6b}$$

von Kármán–Tsien:

$$C_p \approx C_{\text{pinc}} + M_\infty^2 C_{\text{pinc}} (1 - C_{\text{pinc}}/2) \big/ 2 \tag{6c}$$

Strictly speaking, these classical formulas are valid only for two-dimensional flows although they are sometimes used for three-dimensional flows. For a slender body of revolution at zero incidence where the compressibility effect is weaker, the pressure-correction formula based on the linearized theory is[9]

$$C_p \approx C_{\text{pinc}} - \frac{\mathrm{d}^2(R^2)}{\mathrm{d}x^2} \ell n \sqrt{1 - M_\infty^2} \tag{7}$$

where $R(x)$ is the radius of the cross section of the body of revolution.

In higher approximations for solving the nonlinear potential equation, the velocity potential ϕ is expressed by the Janzen–Rayleigh expansion in powers of the Mach number (see Refs. 10 and 11)

$$\phi = U_\infty^2 \left(\phi_0 + M_\infty^2 \phi_1 + \cdots \right) \tag{8}$$

The equations for ϕ_0 and ϕ_1 are $\nabla^2 \phi_0 = 0$ and $\nabla^2 \phi_1 = \nabla \phi_0 \cdot \nabla[(\nabla \phi_0)^2/2]$ with the boundary conditions of zero normal velocity and approaching freestream velocity at infinity. Explicit solutions exist for two simple cases: circular cylinder and sphere.[11] For $M_\infty^2 \ll 1$, the expression for C_p for the cylinder and sphere, respectively, with unit radius are

$$C_p \approx 1 - 4 \sin^2(\theta) - M_\infty^2 4 \sin(\theta)[2 \sin(\theta)/3 - \sin(3\theta)/2]$$

$$C_p \approx 1 - 9 \sin^2(\theta)/4 - M_\infty^2 3 \sin^2(\theta) \times \{0.1924 - 0.2813[1 - \sin^2(\theta)]\} \tag{9}$$

Replacing $\sin^2(\theta)$ by $(1 - C_{\text{pinc}})/4$ and $4(1 - C_{\text{pinc}})/9$ in Eq. (9) for the cylinder and sphere, respectively, we obtain the approximate pressure-correction formulas for $M_\infty^2 \ll 1$:

$$C_p \approx C_{\text{pinc}} + M_\infty^2 \left(2 + C_{\text{pinc}} - 3C_{\text{pinc}}^2\right) \big/ 6$$

$$C_p \approx C_{\text{pinc}} + M_\infty^2 \left(-0.048 + 0.215 C_{\text{pinc}} - 0.167 C_{\text{pinc}}^2\right) \tag{10}$$

For $M_\infty^2 \ll 1$, the pressure-correction formula for two-dimensional flows and axisymmetrical flows can be generally written as

$$C_p \approx C_{\text{pinc}} + M_\infty^2 F(C_{\text{pinc}}) \tag{11}$$

where the correction function $F(C_{\text{pinc}})$ can be approximately expressed as a second-order polynomial $F(C_{\text{pinc}}) = a_0 + a_1 C_{\text{pinc}} + a_2 C_{\text{pinc}}^2$. Given an aerodynamic body, the constant coefficients a_0, a_1, and a_2 can be determined experimentally from pressure tap data. Figure 1 shows the correction function $F(C_{\text{pinc}})$ in different pressure-correction formulas for small Mach numbers. In $C_{\text{pinc}} \in [-1, 1]$, the difference between C_p and C_{pinc} is about 0.05 at $M_\infty = 0.3$ without any pressure correction. For PSP measurements on two-dimensional airfoils, the Prandtl–Glauert rule and von Kármán–Tsien rule are sufficiently accurate to recover the incompressible pressure coefficient. Nevertheless, for complex three-dimensional flows, a general pressure-correction method is required, which provokes the development of the following iterative pressure-correction method. Note that the general Prandtl–Glauert transformation allows pressure correction for a three-dimensional thin wing at the cost of changing the wing aspect ratio. Clearly, changing the wing planform is impractical for wind-tunnel testing.

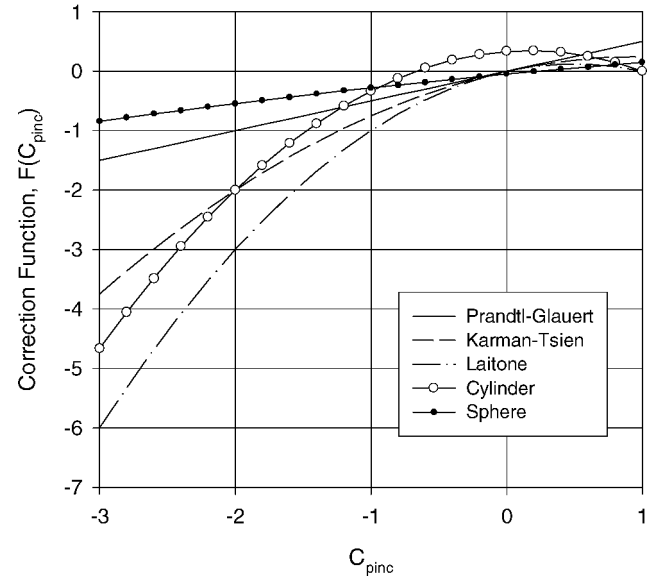

Fig. 1 Correction function $F(C_{\text{pinc}})$ in the classical pressure-correction formulas for small Mach numbers.

Iterative Pressure-Correction Method

The Janzen–Rayleigh method of expansion has been mainly used for potential flows (see Refs. 10 and 11). Nevertheless, the expansion method in powers of the Mach number is generally valid for viscous flows when the Mach number is small. Dimensional analysis of the compressible Navier–Stokes equations indicates that the solution for the velocity field and temperature field depends on the Reynolds number Re, Prandtl number Pr, and Eckert number E. The Eckert number, representing the effect of compressibility, is proportional to M_∞^2. In the case where the Mach number is small and the effects of Reynolds number Re and Prandtl number Pr can be neglected, the velocity field and temperature field can be expanded as a power series of M_∞^2. Accordingly, the pressure field can also be expressed as a power series of M_∞^2. For $M_\infty^2 \ll 1$, in an arbitrary coordinate system, the pressure-correction formula for a three-dimensional surface $Z = S(X, Y)$ has a general functional form

$$C_p \approx C_{\text{pinc}} + M_\infty^2 F[X, Y, S(X, Y)] \tag{12}$$

Equation (12) is valid for not only potential flows, but also for complex viscous flows over a three-dimensional body. Because $C_{\text{pinc}} = C_{\text{pinc}}[X, Y, S(X, Y)]$ is a function of X and Y, we can, in principle, eliminate X in the correction function $F[X, Y, S(X, Y)]$ using C_{pinc} and Y. Because the correction function $F[X, Y, S(X, Y)]$ is not specified yet, an equivalent form to Eq. (12) is written as

$$C_p \approx C_{\text{pinc}} + M_\infty^2 F(C_{\text{pinc}}, Y) \tag{13}$$

Equation (13) indicates that the pressure correction in three-dimensional flows depends on not only C_{pinc}, but also one space coordinate Y. Note that the functional form of Eq. (13) remains

valid after the coordinate Y is switched to another coordinate X. When C_p does not change along one coordinate, Eq. (13) is naturally reduced to Eq. (11) for two-dimensional and axisymmetrical flows.

When the correction function $F(C_{\text{pinc}}, Y)$ is written as a polynomial, Eq. (13) becomes

$$C_p \approx C_{\text{pinc}} + M_\infty^2 \sum_{n=0}^{N} a_n(Y) C_{\text{pinc}}^n \tag{14}$$

Note that C_p and C_{pinc} are functions of the location on the surface $Z = S(X, Y)$, that is, $C_p = C_p[X, Y, S(X, Y)]$ and $C_{\text{pinc}} = C_{\text{pinc}}[X, Y, S(X, Y)]$. When the distributions of C_p and C_{pinc} are known as a function of X along the intersection between the plane $Y = \text{const}$ and the surface $Z = S(X, Y)$, the coefficients $a_n(Y)$ can be determined using the least-squares method. In wind-tunnel measurements, pressure tap data in subsonic compressible flows and the corresponding low-speed flow can be used to establish the relationship between C_p and C_{pinc}. However, this approach is not convenient for PSP measurements in wind tunnels because extra pressure tap data are required. To solve this problem, an iterative method is proposed to recover C_{pinc} from C_p at two different subsonic Mach numbers $M_{\infty 1}$ and $M_{\infty 2}$. The biggest advantage of this method is that C_{pinc} can be directly obtained from two PSP images at $M_{\infty 1}$ and $M_{\infty 2}$ without additional use of pressure tap data.

Denote C_{p1} and C_{p2} as the pressure coefficients at two different Mach numbers $M_{\infty 1}$ and $M_{\infty 2}$ and assume $M_{\infty 1} < M_{\infty 2}$. Given the distributions of C_{p1} and C_{p2} along the intersection between $Y = \text{const}$ and $Z = S(X, Y)$, we need to solve the following equations to recover C_{pinc} and the corresponding coefficients $a_n(Y)$:

$$C_{p1} \approx C_{\text{pinc}} + M_{\infty 1}^2 \sum_{n=0}^{N} a_n(Y) C_{\text{pinc}}^n$$

$$C_{p2} \approx C_{\text{pinc}} + M_{\infty 2}^2 \sum_{n=0}^{N} a_n(Y) C_{\text{pinc}}^n \tag{15}$$

An iteration scheme for solving Eq. (15) is described next:

1) Give the initial distribution $C_{\text{pinc}(k)} = C_{p1}$, $k = 0$, as a function of X along the intersection between $Y = \text{const}$ and $Z = S(X, Y)$ in the object space (a row or column in the image plane), where k is the iteration index number.

2) Determine the coefficients $a_{n(k)}(Y)(n = 0, 1, \ldots, N)$ in the polynomial from a system of equations

$$\frac{\left(C_{p2} - C_{\text{pinc}(k)}\right)}{M_{\infty 2}^2} = \sum_{n=0}^{N} a_{n(k)}(Y) C_{\text{pinc}(k)}^n$$

using the least-squares method.

3) Substitute $a_n(Y)$ into

$$C_{\text{pinc}(k+1)} \approx C_{p1} - M_{\infty 1}^2 \sum_{n=0}^{N} a_{n(k)}(Y) C_{\text{pinc}(k)}^n$$

to obtain the corrected value $C_{\text{pinc}(k+1)}$.

4) Go back to step 2, replace $C_{\text{pinc}(k)}$ by the corrected value $C_{\text{pinc}(k+1)}$ $(k \to k+1)$ and iterate until the converged results $C_{\text{pinc}} = \lim_{k \to \infty} C_{\text{pinc}(k)}$ and $a_n(Y) = \lim_{k \to \infty} a_{n(k)}(Y)$, $n = 0, 1, \ldots, N$, are obtained.

5) Output the final $C_{\text{pinc}} = C_{\text{pinc}}[X, Y, S(X, Y)]$ and $a_n(Y)$.

After processing for a large set of the intersections, we can recover the whole distribution of C_{pinc} on the surface. Unlike the classical pressure-correction methods for two-dimensional flows, the iterative method is a nonlocal approach that has to be done along an intersection. Careful readers may notice that the coordinates of the intersection are not explicitly involved in the described iteration scheme. This implies that the iterative method can be applied to any given line or curve on the surface $Z = S(X, Y)$. Furthermore, it can be directly used in the image plane that has a one-to-one perspective correspondence to the surface $Z = S(X, Y)$. This issue will be discussed in the following section. The selection of the order N of the polynomial in Eq. (15) depends on the complexity of the Mach number effect on the pressure distribution along the intersection. For two-dimensional flows and near-two-dimensional flows, $N = 2$ is sufficient. For more complex flows, the order of the polynomial could be higher. The number of available data points on the intersection eventually limits the order of the polynomial.

Processing in Image Plane

The aforementioned analysis is made in an arbitrary object–space coordinate system (X, Y, Z). For PSP, data processing is typically done in the image plane rather than in the object space. Therefore, it is necessary to discuss the coordinate system and perspective projection mapping because, for convenience, the pressure-correction method should be used in the image plane. Because the preceding analysis does not specify the coordinate system a priori, the coordinate system could be a Cartesian coordinate system, a curvilinear coordinate system, or even a nonorthogonal coordinate system. In this section, we prove that the iterative pressure-correction method can be directly applied to rows or columns in PSP images.

For a given simple solid surface $Z' = S'(X', Y')$ in a Cartesian object space coordinate system (X', Y', Z'), there is a one-to-one perspective projection mapping between the image plane (x, y) and the surface that is imaged by a camera. Hence, a curve on the surface $Z' = S'(X', Y')$ in the object space uniquely maps onto a line on the image plane. Furthermore as shown in Fig. 2, an orthogonal mesh (mesh 1) composed of rows and columns in the image plane has a one-to-one perspective correspondence to a mesh (mesh 2) on the surface $Z' = S'(X', Y')$. Generally, mesh 2 on the surface is nonorthogonal except for a planar surface parallel to the image plane. Next, mesh 2 on surface $Z' = S'(X', Y')$ is orthographically projected to a mesh (mesh 3) on a given plane P in the object space, constituting a two-dimensional nonorthogonal coordinate system (X, Y) on the plane P. Here, the orthographic projection is the perpendicular projection of mesh 2 to the plane P. Thus, mesh 3 with an added coordinate Z normal to the plane P forms a nonorthogonal coordinate system denoted by (X, Y, Z). The surface $Z' = S'(X', Y')$ in the Cartesian coordinate system (X', Y', Z') is described by $Z = S(X, Y)$ in the nonorthogonal coordinate system (X, Y, Z). Precisely speaking, mesh 2 is composed of the intersections between the surface $Z = S(X, Y)$ and the planes $X = \text{const}$ and $Y = \text{const}$. Finally, we establish a one-to-one correspondence between mesh 1 (rows and columns) in the image plane and the intersections between the surface $Z = S(X, Y)$ and the planes $X = \text{const}$ and $Y = \text{const}$ in the nonorthogonal object space coordinate system (X, Y, Z). Consequently, because of this correspondence, the iterative pressure-correction method can be directly applied to PSP images in rows or columns. The pressure correction in the image

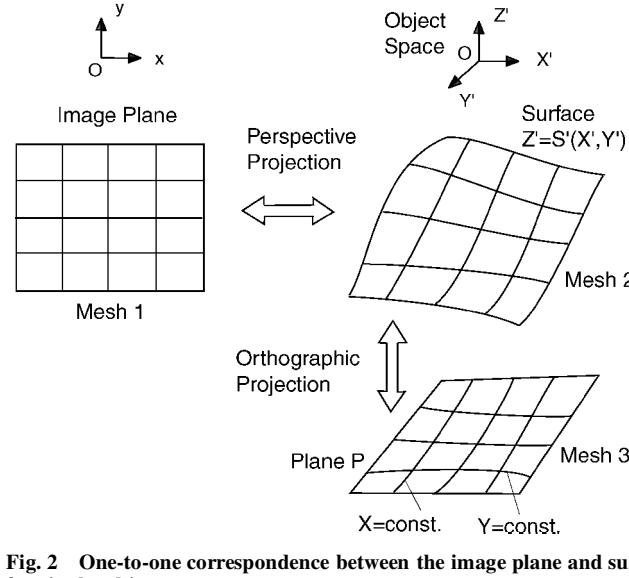

Fig. 2 One-to-one correspondence between the image plane and surface in the object space.

plane considerably simplifies data processing, and it can be easily integrated into current PSP image processing software. In fact, following the same reasoning, one can see that the pressure-correction method can be applied to any given line or curve in the image plane.

Limitations and Uncertainty

There are limitation conditions for application of the iterative pressure-correction method (actually for any pressure-correction method). First, the two Mach numbers $M_{\infty 1}$ and $M_{\infty 2}$ should be lower than the critical Mach number at which the flow at certain point on the surface becomes sonic. Second, the pressure-correction method relies on the assumption that the pressure distribution does not have a drastic change due to the Reynolds number effect as the Mach number increases from $M_\infty = 0$ to $M_{\infty 1}$ and $M_{\infty 2}$. Generally, the pressure coefficient is also a function of the Reynolds number Re, that is,

$$C_p \approx C_{\text{pinc}} + M_\infty^2 F[X, Y, S(X, Y); Re] \tag{16}$$

When the Reynolds number effect on pressure overwhelms the effect of the Mach number, the pressure-correction method cannot produce correct results because the flow pattern has been qualitatively changed. This situation may happen on a high-lift model under certain testing conditions in certain flow separation regions that are particularly sensitive to the Reynolds number effect.[7] Fortunately, there is a large class of flows in which the Reynolds number does not significantly change the surface pressure distribution, such as attached flows and certain separated flows whose separation and reattachment lines are fixed. For these flows, the pressure-correction method is applicable.

To estimate the uncertainty of the iterative pressure-correction method, we consider the iterative relation in step 3 in the preceding section:

$$C_{\text{pinc}(k+1)} = C_{p1} - M_{\infty 1}^2 F\left(C_{\text{pinc}(k)}, Y\right) \tag{17}$$

where k is the iteration index number and the correction function $F(C_{\text{pinc}(k)}, Y)$ is

$$F\left(C_{\text{pinc}(k)}, Y\right) = \sum_{n=0}^{N} a_{n(k)}(Y) C_{\text{pinc}(k)}^n = \frac{\left(C_{p2} - C_{\text{pinc}(k)}\right)}{M_{\infty 2}^2} \tag{18}$$

The uncertainty $\Delta C_{\text{pinc}(k+1)}$ in calculating $C_{\text{pinc}(k+1)}$ at the $(k+1)$ iteration satisfies the error propagation equation derived from Eq. (17),

$$\left(\Delta C_{\text{pinc}(k+1)}\right)^2 = (\Delta C_{p1})^2 + M_{\infty 1}^4 (\Delta F)^2 \tag{19}$$

where ΔC_{p1} is the measurement error of C_{p1} and ΔF is the least-squares estimation error in step 2 for determining the coefficients $a_{n(k)}(Y), n = 0, 1, \ldots, N$, in the polynomial correction function. Furthermore from Eq. (18), we know

$$(\Delta F)^2 = \left[(\Delta C_{p2})^2 + \left(\Delta C_{\text{pinc}(k)}\right)^2\right] M_{\infty 2}^{-4} \tag{20}$$

Therefore, substitution of Eq. (20) into Eq. (19) leads to the following relation:

$$\left(\Delta C_{\text{pinc}(k+1)}\right)^2 = (\Delta C_{p1})^2 + (M_{\infty 1}/M_{\infty 2})^4 \left[(\Delta C_{p2})^2 + \left(\Delta C_{\text{pinc}(k)}\right)^2\right] \tag{21}$$

When the limit $\Delta C_{\text{pinc}} = \lim_{k \to \infty} \Delta C_{\text{pinc}(k)} = \lim_{k \to \infty} \Delta C_{\text{pinc}(k+1)}$ exists, a final estimate for the uncertainty ΔC_{pinc} is

$$(\Delta C_{\text{pinc}})^2 = \left[(\Delta C_{p1})^2 + (M_{\infty 1}/M_{\infty 2})^4 (\Delta C_{p2})^2\right] \times \left[1 - (M_{\infty 1}/M_{\infty 2})^4\right]^{-1} \tag{22}$$

For a fixed ratio of the two Mach numbers $M_{\infty 1}$ and $M_{\infty 2}$, the computational uncertainty ΔC_{pinc} is mainly determined by the errors of the given pressure-coefficient distributions C_{p1} and C_{p2}. Equation (22) indicates that the Mach numbers $M_{\infty 1}$ and $M_{\infty 2}$ should be considerably different. When $M_{\infty 1}$ approaches to $M_{\infty 2}$, the uncertainty ΔC_{pinc} is rapidly increased.

Test Cases

Cylinder and Sphere

To validate the iterative pressure-correctionmethod, we first consider classical cases: flows over a circular cylinder and sphere. Figure 3 shows the incompressible C_{pinc} distribution on a cylinder recovered by using the iterative pressure-correction method along with results obtained by using the Prandtl–Glauert rule and von Kármán–Tsien rule. The iterative method gives excellent recovery of C_{pinc}. The von Kármán–Tsien rule also gives a good correction, whereas the Prandtl–Glauert rule is not accurate in the low-pressure region $C_p \in [-3, -2]$. The iterative method uses the distributions of C_p at $M_{\infty 1} = 0.4$ and $M_{\infty 2} = 0.6$. The order of the polynomial in Eq. (15) is $N = 2$, and the solution for C_{pinc} converges after 10 iterations. Both the von Kármán–Tsien rule and Prandtl–Glauert rule use C_p at $M_\infty = 0.4$ to recover C_{pinc}. Figure 4 shows recovery of the incompressible C_{pinc} distribution on the sphere. Again, the iterative method produces excellent results. Interestingly, in contrast to the flow over the two-dimensional cylinder, the Prandtl–Glauert rule works better than the von Kármán–Tsien rule in this three-dimensional case, where the compressibility effect is much weaker. Certainly, for two-dimensional subsonic flows, the von Kármán–Tsien rule derived from the two-dimensional nonlinear potential equation is more accurate than the Prandtl–Glauert rule. However,

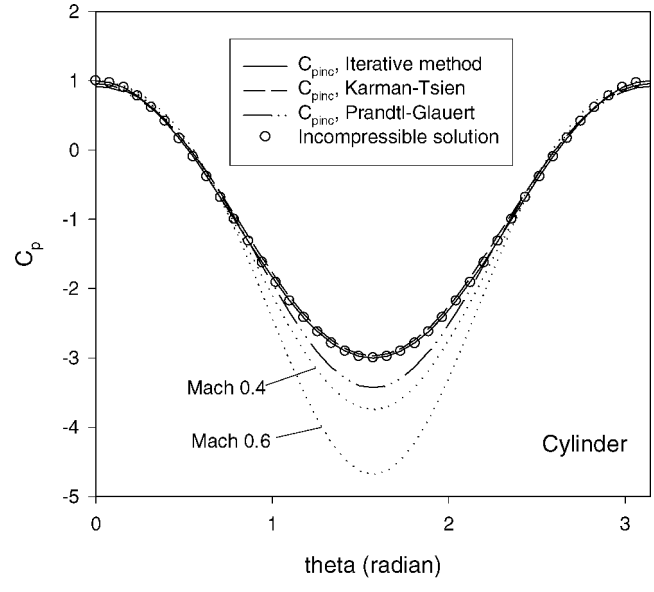

Fig. 3 Pressure correction for cylinder.

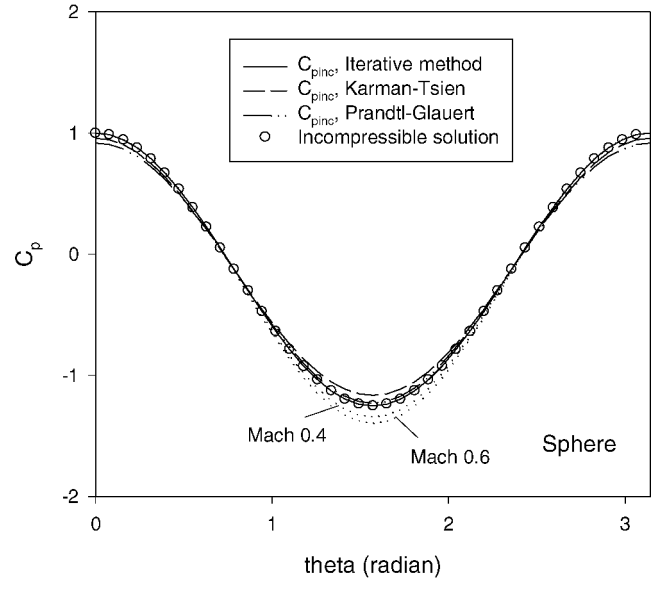

Fig. 4 Pressure correction for sphere.

the accuracy of the von Kármán–Tsien rule is not assured for three-dimensional flows.

Prolate Spheroid and Transonic Body

Figure 5a shows the pressure correction for a prolate spheroid of fineness ratio 6 at an angle of attack of 5.6 deg and the ellipsoidal coordinate $\omega = 0$. Here, the iterative method uses C_p data at $M_{\infty 1} = 0.6$ and $M_{\infty 2} = 0.8$ that are collected from the scanned figures in Ref. 12. Even though the Mach numbers are not small, the iterative method still produces good results because these Mach numbers are less than the critical Mach number of 0.904 in this case. Figure 5b shows similar pressure correction for a transonic body at zero angle of attack.[12] In Ref. 12, data at $M_\infty = 0$ were obtained by directly extrapolating the pressure coefficients at higher Mach numbers to the Mach number of zero. The accuracy of this simple extrapolation is not known. Because the measurement uncertainty of the pressure coefficient is not provided in Ref. 12, we cannot directly use Eq. (22) to give the uncertainty of the iterative pressure-correction method. Nevertheless, under certain assumptions, a rough estimate for the uncertainty ΔC_{pinc} can be given based on the least-squares estimation error ΔF in step 2. Under the assumptions that $(M_{\infty 1}/M_{\infty 2})^4 \ll 1$ and $\Delta C_{p1} \approx \Delta C_{p2}$, when the iteration converges, comparing Eq. (19) with Eq. (22) yields a rough estimate:

$$(\Delta C_{p1})^2 \Big/ M_{\infty 1}^4 (\Delta F)^2 \approx (M_{\infty 2}/M_{\infty 1})^4 \tag{23}$$

When the iteration index k is large enough, substitution of Eq. (23) into Eq. (19) leads to

$$(\Delta C_{\text{pinc}})^2 \approx \left(M_{\infty 1}^4 + M_{\infty 2}^4\right)(\Delta F)^2 \tag{24}$$

The error bars on the calculated curves of C_{pinc} in Fig. 5 show the uncertainty ΔC_{pinc} estimated using Eq. (24).

Delta Wing

To examine the capability of the iterative pressure-correction method for complex vortical flows where two-dimensional methods cannot be used, it is used to recover C_{pinc} on the upper surface of a 65-deg delta wing with a sharp leading edge.[13] Figure 6 shows the spanwise C_{pinc} distributions obtained using the iterative method at the chordwise locations $x/cr = 0.6$ and $x/cr = 0.8$ at an angle of attack (AOA) of 20.5 deg, where cr is the root chord of the wing. In Fig. 6, C_p data at $M_{\infty 1} = 0.4$ and $M_{\infty 2} = 0.6$ are used for the iterative pressure correction. Because the Mach number effect on the pressure distribution is more complicated in this case, we choose the order of the polynomial $N = 8$ with 20 iterations. Data at Mach 0.4 and 0.6 are obtained from tests on a 65-deg delta wing with a root chord of 25.734 in. and a wingspan of 24 in. in the NASA Langley

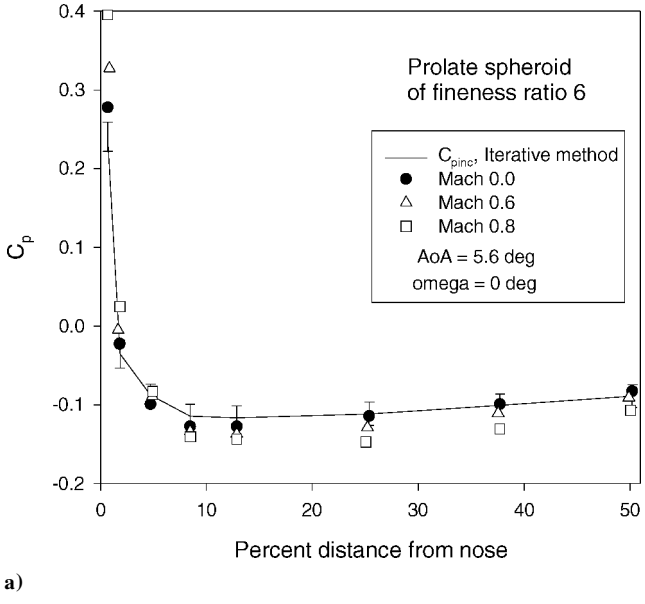

a)

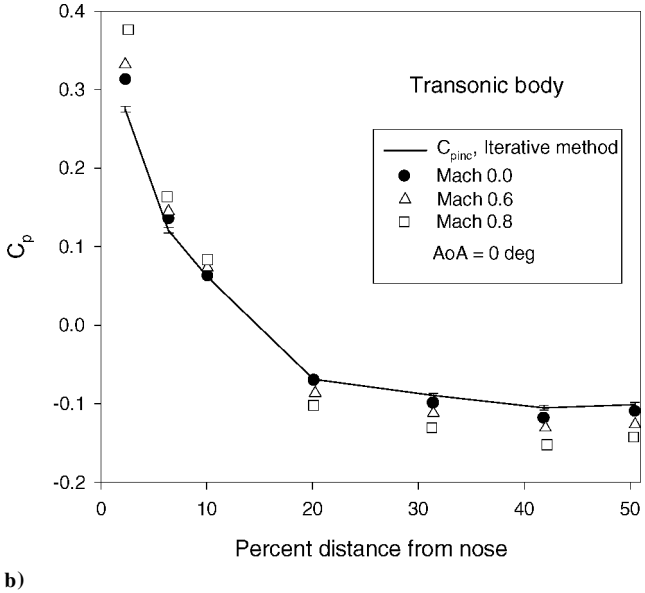

b)

Fig. 5 Pressure correction for a) prolate spheroid and b) transonic body.

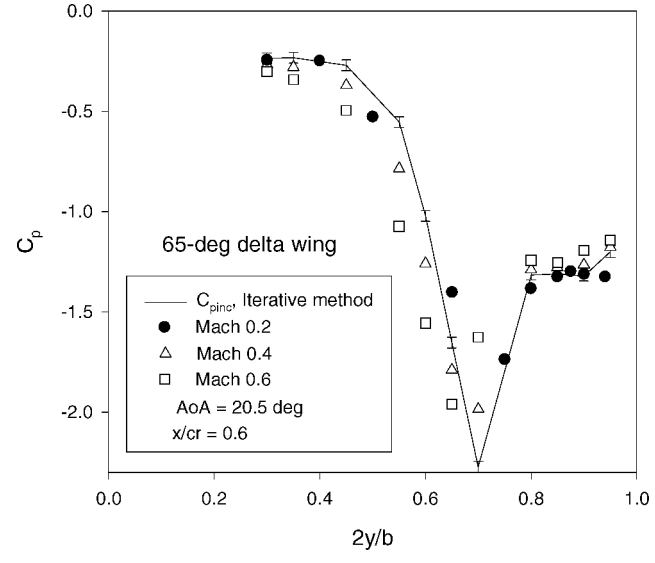

a)

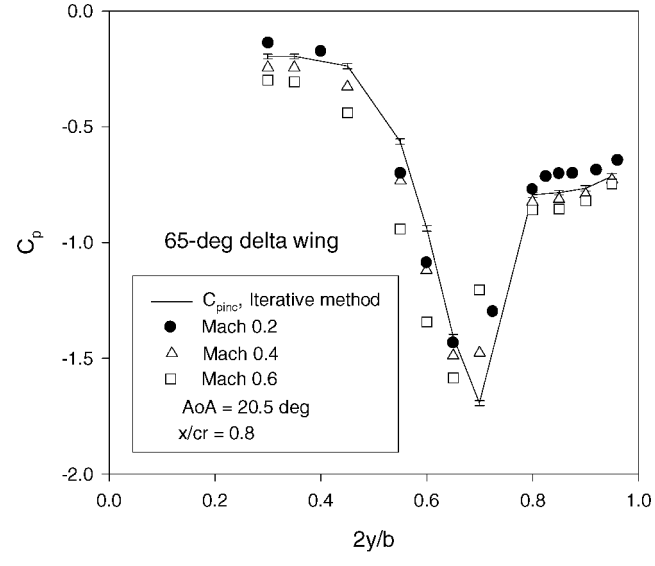

b)

Fig. 6 Spanwise pressure correction for a 65-deg delta wing at an AOA of 20.5 deg at two chordwise locations: a) $x/cr = 0.6$ and b) $x/cr = 0.8$.

Research Center National Transonic Facility (NTF).[13] Because low-speed pressure data are not available in the same NTF tests, data at Mach 0.2 and the same nominal AOA on a smaller 65-deg delta wing with cut tips obtained in the NASA Langley Research Center Basic Aerodynamics Research Tunnel (BART) are used for comparison. The error bars on the calculated curves of C_{pinc} in Fig. 6 show the computational uncertainty ΔC_{pinc}. The recovered distributions of C_{pinc} show the correct trend as the Mach number increases.[13–15]

In this paper, the pressure-correction method is not directly applied to actual PSP data because the author does not have PSP images at suitable subsonic Mach numbers and the corresponding reliable incompressible results for comparison. To validate this new concept, however, it is appropriate to apply this method to a number of classical flows for pressure tap data. Future research will focus on the use of the iterative pressure-correction method in PSP measurements at low speeds.

Conclusions

The iterative pressure-correction method is developed for low-speed PSP measurements in three-dimensional flows. This method is based on a general expansion of the pressure coefficient in powers of the freestream Mach number. The pressure-correction function, which is modeled by a polynomial, is determined using an iteration scheme. This method can recover the incompressible pressure-coefficient distribution from PSP images obtained at two different subsonic Mach numbers. Unlike the classical pressure-correction formulas, the iterative pressure-correction method can be used in general three-dimensional flows. The computational uncertainty of the method is mainly a result of the errors of the given pressure-coefficient distributions at higher Mach numbers. Without pushing a PSP system to the limit, the pressure-correction methodology allows the extension of the current PSP technique to a large class of low-speed flows where the surface pressure field is not sensitive to the Reynolds number. This method is validated for flows over a number of basic aerodynamic configurations.

Acknowledgments

The author thanks J. P. Sullivan, J. H. Bell, and the reviewers for their comments.

References

[1]Liu, T., Guille, M., and Sullivan, J., "Accuracy of Pressure-Sensitive Paint," *AIAA Journal*, Vol. 39, No. 1, 2001, pp. 103–112.

[2]Brown, O. C., "Low-Speed Pressure Measurements Using a Luminescent Coating System," Ph.D. Dissertation, Dept. of Aeronautics and Astronautics, Stanford Univ. Stanford, CA, May 2000.

[3]Morris, M. J., "Use of Pressure-Sensitive Paints in Low-Speed Flows," *Proceedings of the 16th International Congress on Instrumentation in Aerospace Simulation Facilities*, Inst. of Electrical and Electronics Engineers, Dayton, OH, 1995, pp. 31.1–31.10.

[4]Shimbo, Y., Mehta, R. D., and Cantwell, B. J., "Vortical Flow Field Investigation Using the Pressure Sensitive Paint Technique," AIAA Paper 97-0388, Jan. 1997.

[5]Le Sant, Y., Bouvier, F., Merienne, M.-C., and Peron, J.-L., "Low Speed Tests Using PSP at ONERA," AIAA Paper 2001-0555, Jan. 2001.

[6]Applin, Z. T., "Pressure Distributions from Subsonic Tests of a NACA 0012 Semispan Wing Model," NASA TM-110148, Sept. 1995.

[7]Applin, Z. T., Gentry, G. L., and Takallu, M. A., "Wing Pressure Distributions from Subsonic Tests of a High-Wing Transport Model," NASA TM-4583, Jan. 1995.

[8]Anderson, J., *Modern Compressible Flow*, 2nd ed., McGraw–Hill, New York, 1990, pp. 242–293.

[9]Sears, W. R., "Small Perturbation Theory," *General Theory of High Speed Aerodynamics*, edited by W. R. Sears, Princeton Univ. Press, Princeton, NJ, 1954, pp. 61–119.

[10]Kaplan, C., The Flow of a Compressible Fluid past a Curved Surface, NACA TR-768, Sept. 1943.

[11]Lighthill, M. J., "Higher Approximations," *General Theory of High Speed Aerodynamics*, edited by W. R. Sears, Princeton Univ. Press, Princeton, NJ, 1954, pp. 345–489.

[12]Matthews, C. W., "A Comparison of the Experimental Subsonic Pressure Distributions About Several Bodies of Revolution with Pressure Distributions Computed by Means of the Linearized Theory," NACA TR-1155, Nov. 1951.

[13]Chu, J., and Luckring, J. M., "Experimental Surface Pressure Data Obtained on 65° Delta Wing Across Reynolds Number and Mach Number Ranges," *Sharp Leading Edge*, Vol. 1, NASA TM-4645, Feb. 1996.

[14]Wendt, J. F., "Compressibility Effects on Flows around Simple Components," *Introduction to Vortex Dynamics*, Lecture Series 1986-08, von Kármán Inst. for Fluid Mechanics, Rhode-Saint-Genese, Belgium, 1986, pp. 7-1–7-20.

[15]Vorropoulos, G., and Wendt, J. F., (1986), "Compressibility Effects on Delta Wing Flow Fields," *Introduction to Vortex Dynamics*, Lecture Series 1986-08, von Kármán Inst. for Fluid Mechanics, Rhode-Saint-Genese, Belgium, 1986, pp. 1–14.

R. P. Lucht
Associate Editor